Organometallics **1998,** *17,* 255−261

New Synthesis of $[SFe_3(CO)_9]^{2-}$ and Its Reactivity toward Electrophiles

Jiann-Jang Cherng,[†] Yi-Chou Tsai,[†] Chuen-Her Ueng,[†] Gene-Hsiang Lee,[‡]
Shie-Ming Peng,[§] and Minghuey Shieh*[,†]

Department of Chemistry, National Taiwan Normal University, Taipei 11718, Taiwan, Republic of China, and Instrumentation Center and Department of Chemistry, National Taiwan University, Taipei 10764, Taiwan, Republic of China

Received August 12, 1997

The reaction of Na_2SO_3 with $Fe(CO)_5$/KOH in methanol forms the tetrahedral cluster $[SFe_3(CO)_9]^{2-}$ in good yield. Acidification of $[SFe_3(CO)_9]^{2-}$ with H^+ forms the monohydrido cluster $[SFe_3(\mu\text{-}H)(CO)_9]^-$ (**I**) and the dihydrido cluster $SFe_3(\mu\text{-}H)_2(CO)_9$. Further methylation of $[SFe_3(CO)_9]^{2-}$ with $MeSO_3CF_3$ produces the sulfur-methylated cluster $[MeSFe_3(CO)_9]^-$ (**II**). When $[SFe_3(CO)_9]^{2-}$ is treated with $Ru_3(CO)_{12}$ in refluxing acetone, the octahedral cluster $[SFe_2Ru_3(CO)_{14}]^{2-}$ (**III**) is obtained. Subsequent methylation of **III** with $MeSO_3CF_3$ gives the octahedral cluster $[MeSFe_2Ru_3(CO)_{14}]^-$ (**IV**), in which the sulfur atom is pentacoordinated to one methyl group and two Ru and two Fe atoms. Clusters **I**−**IV** have been fully structurally characterized by spectroscopic methods and X-ray analysis. In this paper, the basic sites of $[SFe_3(CO)_9]^{2-}$ are studied in terms of the differing electrophiles, and a novel pentacoordinate bonding mode of the sulfur atom is also found in cluster **IV**.

Introduction

Transition-metal carbonyl clusters containing p-block elements have attracted great attention due to their interesting bonding modes and versatile structural features.[1] Recently, the rich chemistry of transition-metal chalcogenides[2] and our interest in iron−selenium and −tellurium clusters[3] prompted us to explore the sulfur-containing metal carbonyl clusters. Bridging sulfido ligands have been shown to be effective ligands in the stabilization of polynuclear transition-metal clusters, and they also adopt a variety of coordination modes, including μ_2, μ_3, and μ_4.[4]

Although quite a few organometallic metal-sulfide clusters are known, the synthetic routes have often not been well-developed.[4] Of the iron−sulfur−carbonyl clusters, the μ_3-sulfido tetrahedral cluster $[SFe_3(CO)_9]^{2-}$ is known and some synthetic routes have been reported; however, a convenient preparation was not available.[5] To compare its reactivity with those of its analogs $[EFe_3(CO)_9]^{2-}$ (E = Se, Te),[3g,6] we have developed a new synthesis of $[SFe_3(CO)_9]^{2-}$ and have studied its further reactions with some electrophiles such as HCl, CH_2I_2, CF_3SO_3Me, and $Ru_3(CO)_{10}(Me_2CO)_2$. Structural features of the resultant new clusters $[SFe_3(\mu\text{-}H)(CO)_9]^-$ (**I**), $[MeSFe_3(CO)_9]^-$ (**II**), and $[SFe_2Ru_3(CO)_{14}]^{2-}$ (**III**) are described. The sulfur-methylated cluster $[MeSFe_2Ru_3(CO)_{14}]^-$ (**IV**) with a pentacoordinate sulfido ligand is also described.

Experimental Section

All reactions were performed under an atmosphere of pure nitrogen using standard Schlenk techniques.[7] Solvents were purified, dried, and distilled under nitrogen prior to use. Infrared spectra were recorded on a Jasco 5300 or a Perkin-Elmer Paragon 500 IR spectrometer as solutions in CaF_2 cells. ESI (electron spray ionization) mass spectra were obtained on a JMS D-300 mass spectrometer using MeCN as the solvent in cent mode. The ^1H and ^{13}C NMR spectra were taken on a JEOL 400 instrument at 399.78 and 100.53 MHz, respectively. Elemental analyses of C, H, and N were performed on a Perkin-Elmer 2400 analyzer at the NSC Regional Instrumental Center at National Taiwan University, Taipei, Taiwan.

---

* To whom all correspondence should be addressed.

[†] Department of Chemistry, National Taiwan Normal University.

[‡] Instrumentation Center, National Taiwan University.

[§] Department of Chemistry, National Taiwan University.

(1) (a) Johnson, B. F. G. *Transition Metal Clusters*; Wiley: New York, 1980. (b) Shriver, D. F.; Kaesz, H. D.; Adams, R. D. *The Chemistry of Metal Cluster Complexes*; VCH: New York, 1990. (c) Mingos, D. M. P.; Wales, D. J. *Introduction to Cluster Chemistry*; Prentice Hall: Englewood Cliffs, NJ, 1990.

(2) (a) Linford, L.; Raubenheimer, H. G. *Adv. Organomet. Chem.* **1991**, *32*, 1. (b) Roof, L. C.; Kolis, J. W. *Chem. Rev.* **1993**, *93*, 1037. (c) Bogan, L. E.; Rauchfuss, T. B.; Rheingold, A. L. *J. Am. Chem. Soc.* **1985**, *107*, 3843. (d) Mathur, P.; Mavunkal, I. J.; Rugmini, V.; Mahon, M. F. *Inorg. Chem.* **1990**, *29*, 4838.

(3) (a) Shieh, M.; Chen, P.-F.; Peng, S.-M.; Lee, G.-H. *Inorg. Chem.* **1993**, *32*, 3389. (b) Shieh, M.; Shieh, M.-H. *Organometallics* **1994**, *13*, 920. (c) Shieh, M.; Tsai, Y.-C. *Inorg. Chem.* **1994**, *33*, 2303. (d) Shieh, M.; Shieh, M.-H.; Tsai, Y.-C.; Ueng, C.-H. *Inorg. Chem.* **1995**, *34*, 5088. (e) Shieh, M.; Chen, P.-F.; Tsai, Y.-C.; Shieh, M.-H.; Peng, S.-M.; Lee, G.-H. *Inorg. Chem.* **1995**, *34*, 2251. (f) Shieh, M.; Tang, T.-F.; Peng, S.-M.; Lee, G.-H. *Inorg. Chem.* **1995**, *34*, 2797. (g) Shieh, M.; Tsai, Y.-C.; Cherng, J.-J.; Shieh, M.-H.; Chen, H.-S.; Ueng, C.-H. *Organometallics* **1997**, *16*, 456.

(4) (a) Adams, R. D.; Tsai, M. *J. Cluster Sci.* **1990**, *1*, 249. (b) Adams, R. D. *Polyhedron* **1985**, *4*, 2003. (c) Vahrenkamp, H. *Angew. Chem., Int. Ed. Engl.* **1975**, *14*, 322.

(5) (a) Markó, L.; Takács, J.; Papp, S.; Markó-Monostory, B. *Inorg. Chim. Acta* **1980**, *45*, L189. (b) Markó, L.; Takács, J. *Inorg. Synth.* **1989**, *26*, 243. (c) Fischer, K.; Deck, W.; Schwarz, M.; Vahrenkamp, H. *Chem. Ber.* **1985**, *118*, 4946. (d) Holliday, R. L.; Roof, L. C.; Hargus, B.; Smith, D. M.; Wood, P. T.; Pennington, W. T.; Kolis, J. W. *Inorg. Chem.* **1995**, *34*, 4392.

(6) (a) Roof, L. C.; Smith, D. M.; Drake, G. W.; Pennington, W. T.; Kolis, J. W. *Inorg. Chem.* **1995**, *34*, 337. (b) Bachman, R. E.; Whitmire, K. H.; van Hal, J. *Organometallics* **1995**, *14*, 1792.

(7) Shriver, D. F.; Drezdzon, M. A. *The Manupulation of Air Sensitive Compounds*; Wiley: New York, 1986.

S0276-7333(97)00710-3 CCC: $15.00

Table 1. Crystallographic Data for $[Et_4N][SFe_3(\mu\text{-}H)(CO)_9]$ ($[Et_4N][\textbf{I}]$), $[Et_4N][MeSFe_3(CO)_9]$($[Et_4N][\textbf{II}]$), $[Et_4N]_2[SFe_2Ru_3(CO)_{14}]$ ($[Et_4N]_2[\textbf{III}]$), and $[Et_4N][MeSFe_2Ru_3(CO)_{14}]$ ($[Et_4N][\textbf{IV}]$)

	$[Et_4N][\textbf{I}]$	$[Et_4N][\textbf{II}]$	$[Et_4N]_2[\textbf{III}]$	$[Et_4N][\textbf{IV}]$
formula	$C_{17}H_{21}Fe_3NO_9S$	$C_{18}H_{23}Fe_3NO_9S$	$C_{30}H_{40}Fe_2N_2O_{14}Ru_3S$	$C_{23}H_{23}Fe_2NO_{14}Ru_3S$
fw	581.95	596.98	1101.80	986.67
cryst syst	triclinic	orthorhombic	monoclinic	monoclinic
space group	$P\bar{1}$	*Pmcn*	$P2_1/c$	*Cc*
a, Å	8.609(3)	11.514(2)	16.708(5)	9.838(3)
b, Å	12.060(3)	12.748(4)	11.448(3)	28.402(5)
c, Å	12.472(3)	17.030(2)	22.113(4)	11.839(2)
α, deg	77.58(2)			
β, deg	80.41(3)		107.11(3)	92.05(2)
γ, deg	72.91(3)			
V, Å^3	1201.3(6)	2499.5(9)	4042.5(2)	3306.1(1)
Z	2	4	4	4
D(calc), M gm^{-3}	1.609	1.586	1.549	2.111
abs coeff, cm^{-1}	19.144	18.4	18.860	22.9
diffractometer	Nonius (CAD-4)	Nonius (CAD-4)	Nonius (CAD-4)	Nonius (CAD-4)
λ(Mo Kα), Å	0.7107	0.7107	0.7107	0.7107
temp, °C	25	25	25	25
T_{min}/T_{max}	0.81/1.00	0.76/1.00	0.66/1.00	0.81/1.00
residues:[a] *R*; R_w	0.026; 0.025	0.040; 0.034	0.054; 0.049	0.047; 0.042

[a] The functions minimized during least-squares cycles were $R = \Sigma|F_o - F_c|/\Sigma F_o$ and $R_w = [\Sigma w(F_o - F_c)^2/\Sigma w(F_o)^2]^{1/2}$.

Synthesis of $[Et_4N]_2[SFe_3(CO)_9]$. To a sample of 0.318 g (2.52 mmol) of Na_2SO_3 and 1.583 g of KOH (28.2 mmol) was added 1.00 mL of $Fe(CO)_5$ (7.61 mmol) and 40 mL of MeOH. The mixture was heated to reflux for 4 days, the resultant solution was filtered, and 1.73 g (8.23 mmol) of $[Et_4N]Br$ was added to the filtrate to precipitate the red-brown products. The solid was then washed with H_2O and Et_2O several times and extracted with MeCN and the extract recrystallized with Et_2O/MeCN to give 0.58 g (0.81 mmol) of $[Et_4N]_2[SFe_3(CO)_9]$[5] (33% based on S). IR (ν(CO), MeCN): 1999 w, 1931 vs, 1904 m, 1874 w cm^{-1}.

Reaction of $[Et_4N]_2[SFe_3(CO)_9]$ with HCl(aq). To a sample of 0.365 g (0.512 mmol) of $[Et_4N]_2[SFe_3(CO)_9]$ in 20 mL of MeCN in an ice−water bath was added dropwise 1.5 mL of 4 M HCl(aq). The mixture was stirred in an ice−water bath for 10 min, then warmed to room temperature, and stirred for another 5 h. The resultant solution was filtered, and the solvent was removed under vacuum. The residue was washed with deionized water several times and then extracted with hexanes. The hexane extract was shown to be the known compound $SFe_3(\mu\text{-}H)_2(CO)_9$.[5a] The yield was 0.010 g (0.022 mmol, 4.3% based on S). IR (ν(CO), hexane): 2106 m, 2069 vs, 2050 vs, 2039 vs, 2034 s, 2013 vs, 2001 s, 1993 m, 1986 m cm^{-1}. ^{1}H NMR ($CDCl_3$, 298 K, ppm): −24.51 (s). The CH_2Cl_2 extract was recrystallized with hexanes/CH_2Cl_2 to give 0.14 g (0.24 mmol) of the previously reported complex $[Et_4N][SFe_3(\mu\text{-}H)(CO)_9]$[5a] ($[Et_4N][\textbf{I}]$) (47% based on S). IR ($\nu$(CO), CH_2Cl_2): 2052 w, 2009 vs, 1982 vs, 1965 s, 1950 m, sh, 1914 w cm^{-1}. ^{1}H NMR (DMSO-d_6, 298 K, ppm): −22.93 (s) (chemical shifts not given for $[Et_4N]^+$). Crystals of $[Et_4N][\textbf{I}]$ suitable for X-ray analysis were grown from hexanes/CH_2Cl_2 solutions.

Reaction of $[Et_4N]_2[SFe_3(CO)_9]$ with CH_2I_2. To 0.434 g (0.609 mmol) of $[Et_4N]_2[SFe_3(CO)_9]$ in 20 mL of MeCN in an ice−water bath was added dropwise 0.1 mL (1.24 mmol) of CH_2I_2. The mixture was stirred in an ice−water bath for 30 min and then warmed to room temperature and stirred for 18 h. The resultant solution was filtered to collect the filtrate, and the solvent was removed under vacuum. The residue was extracted with hexanes; the extract was then chromatographed to give a trace amount of $S_2Fe_3(CO)_9$. The CH_2Cl_2 extract was shown by IR to be $[SFe_3(\mu\text{-}H)(CO)_9]^-$ (**I**). The yield was 0.190 g (0.326 mmol, 54% based on S).

Reaction of $[Et_4N]_2[SFe_3(CO)_9]$ with CF_3SO_3Me. To 0.458 g (0.643 mmol) of $[Et_4N]_2[SFe_3(CO)_9]$ in 30 mL of CH_2Cl_2 in an ice−water bath was added dropwise 0.15 mL (1.33 mmol) of CF_3SO_3Me. The mixture was stirred in an ice−water bath for 1.5 h. The resultant solution was filtered to collect the filtrate, and the solvent was removed under vacuum. The residue was extracted with hexanes and then with THF. The THF extract was recrystallized with hexanes/CH_2Cl_2 to give 0.33 g (0.536 mmol) of $[Et_4N][MeSFe_3(CO)_9]$ ($[Et_4N][\textbf{II}]$) (83% based on $[Et_4N]_2[SFe_3(CO)_9]$). IR (ν(CO), CH_2Cl_2): 2033 s, 1971 vs, 1943 s, 1918 s cm^{-1}. Anal. Calcd for $[Et_4N][MeSFe_3(CO)_9]$: C, 36.22; H, 3.88; N, 2.35. Found: C, 36.01; H, 3.67; N, 2.33. ESI mass: M$^-$ at *m*/*e* 466. ^{1}H NMR (MeCN-d_3, 298 K, ppm): 2.73 (s) (chemical shifts not given for $[Et_4N]^+$). ^{13}C NMR (MeCN-d_3, 298 K, ppm): 53.2, 218.5 (chemical shifts not given for $[Et_4N]^+$).

Reaction of $[Et_4N]_2[SFe_3(CO)_9]$ with $Ru_3(CO)_{12}$. To a mixture of 0.356 g (0.500 mmol) of $[Et_4N]_2[SFe_3(CO)_9]$ and 0.346 g (0.54 mmol) of $Ru_3(CO)_{12}$ was added 40 mL of Me_2CO. The mixture was heated to reflux for 8.5 h, the resultant solution was filtered, and the solvent was removed under vacuum to give an oily residue. The CH_2Cl_2 extract was recrystallized with hexanes/CH_2Cl_2 to give 0.48 g (0.44 mmol) of the pure compound $[Et_4N]_2[SFe_2Ru_3(CO)_{14}]$ ($[Et_4N]_2[\textbf{III}]$) (87% based on $[Et_4N]_2[SFe_3(CO)_9]$). IR (ν(CO), CH_2Cl_2): 2029 w, 1973 vs, 1917 sh, 1763 m, br cm^{-1}. ^{13}C NMR (DMSO-d_6, 298 K, ppm): 209.9 (chemical shifts not given for $[Et_4N]^+$). Anal. Calcd for $[Et_4N]_2[SFe_2Ru_3(CO)_{14}]$: C, 32.77; H, 3.67; N, 2.55. Found: C, 32.91; H, 3.69; N, 2.64. ESI mass: M$^-$ at *m*/2*e* (^{102}Ru) 420. Crystals suitable for X-ray diffraction were grown from hexanes/CH_2Cl_2 solutions.

Reaction of $[Et_4N]_2[SFe_2Ru_3(CO)_{14}]$ ($[Et_4N]_2[\textbf{III}]$) with CF_3SO_3Me. To a solution of 0.500 g (0.45 mmol) of $[Et_4N]_2[\textbf{III}]$ in 35 mL of CH_2Cl_2 in an ice−water bath was added dropwise 0.2 mL of CF_3SO_3Me. The mixture was stirred in the ice−water bath for 1 h and then stirred at room temperature for 2 days. The resultant solution was filtered, and the solvent was removed under vacuum. The CH_2Cl_2 extract was recrystallized with hexanes/CH_2Cl_2 to give 0.37 g (0.36 mmol) of the pure compound $[Et_4N][MeSFe_2Ru_3(CO)_{14}]$ ($[Et_4N][\textbf{IV}]$) (83% based on $[Et_4N]_2[SFe_2Ru_3(CO)_{14}]$). IR ($\nu$(CO), CH_2Cl_2): 2052 w, 1998 vs, 1948 m, 1792 w br cm^{-1}. Crystals suitable for X-ray diffraction were grown from hexanes/CH_2Cl_2 solutions. Anal. Calcd for $[Et_4N][MeSFe_2Ru_3(CO)_{14}]$: C, 28.06; H, 2.36; N, 1.42. Found: C, 28.26; H, 2.44; N, 1.48. Mass (ESI): M$^-$ at *m*/*e* (^{102}Ru) 856. ^{1}H NMR (DMSO-d_6, 298 K, ppm): 2.36 (s) (chemical shifts not given for $[Et_4N]^+$). ^{13}C NMR (DMSO-d_6, 298 K, ppm): 49.7, 205.2 (chemical shifts not given for $[Et_4N]^+$).

X-ray Structural Characterization of the Complexes $[Et_4N][\textbf{I}]$, $[Et_4N][\textbf{II}]$, $[Et_4N]_2[\textbf{III}]$, and $[Et_4N][\textbf{IV}]$. A summary of selected crystallographic data for $[Et_4N][\textbf{I}]$, $[Et_4N][\textbf{II}]$, $[Et_4N]_2[\textbf{III}]$, and $[Et_4N][\textbf{IV}]$ is given in Table 1. Data collection was carried out on a Nonius CAD-4 diffractometer using

Table 2. Selected Bond Distances (Å) and Bond Angles (deg) for $[Et_4N][SFe_3(\mu\text{-}H)(CO)_9]$ ($[Et_4N][I]$)

(A) Distances			
Fe(1)−Fe(2)	2.5730(9)	Fe(1)−Fe(3)	2.668(1)
Fe(1)−S	2.203(1)	Fe(1)−H	1.63(3)
Fe(2)−Fe(3)	2.579(1)	Fe(2)−S	2.191(1)
Fe(3)−S	2.193(1)	Fe(3)−H	1.52(3)
(B) Angles			
Fe(2)−Fe(1)−Fe(3)	58.93(3)	Fe(2)−Fe(1)−S	53.94(4)
Fe(2)−Fe(1)−H	78.3(10)	Fe(3)−Fe(1)−S	52.46(3)
Fe(3)−Fe(1)−H	30.9(10)	S−Fe(1)−H	83.1(10)
Fe(1)−Fe(2)−Fe(3)	62.36(3)	Fe(1)−Fe(2)−S	54.38(3)
Fe(3)−Fe(2)−S	53.99(3)	Fe(1)−Fe(3)−Fe(2)	58.71(3)
Fe(1)−Fe(3)−S	52.82(3)	Fe(1)−Fe(3)−H	33.5(11)
Fe(2)−Fe(3)−S	53.93(3)	Fe(2)−Fe(3)−H	79.9(11)
S−Fe(3)−H	86.0(11)	Fe(1)−S−Fe(2)	71.68(4)
Fe(1)−S−Fe(3)	74.72(4)	Fe(2)−S−Fe(3)	72.08(4)
Fe(1)−H−Fe(3)	115.6(18)		

Table 3. Selected Bond Distances (Å) and Bond Angles (deg) for $[Et_4N][MeSFe_3(CO)_9]$ ($[Et_4N][II]$)

(A) Distances			
Fe(1)−Fe(1a)	2.642(2)	Fe(1)−Fe(2)	2.632(1)
Fe(1)−S	2.127(2)	Fe(2)−S	2.124(2)
S−C(6)	1.836(7)		
(B) Angles			
Fe(1a)−Fe(1)−Fe(2)	59.88(3)	Fe(1a)−Fe(1)−S	51.62(4)
Fe(2)−Fe(1)−S	51.68(5)	Fe(1)−Fe(2)−Fe(1a)	60.25(3)
Fe(1)−Fe(2)−S	51.81(4)	Fe(1a)−Fe(2)−S	51.81(4)
Fe(1)−S−Fe(1a)	76.77(7)	Fe(1)−S−Fe(2)	76.51(6)

graphite-monochromated Mo Kα radiation at 25 °C and employing the $\theta/2\theta$ scan mode. A ψ scan absorption correction was made.[8] All crystals were mounted on glass fibers with epoxy cement. Data reduction and structural refinement were performed using the NRCC-SDP-VAX packages,[9] and atomic scattering factors were taken from ref 10.

Structures of $[Et_4N][I]$, $[Et_4N][II]$, $[Et_4N]_2[III]$, and $[Et_4N][IV]$. The black crystal of $[Et_4N][\mathbf{I}]$ chosen for diffraction measurement was ca. 0.30 × 0.40 × 0.40 mm, the black crystal of $[Et_4N][\mathbf{II}]$ had dimensions 0.50 × 0.35 × 0.20 mm, the crystal of $[Et_4N]_2[\mathbf{III}]$ had dimensions 0.01 × 0.30 × 0.40 mm, and the black crystal of $[Et_4N][\mathbf{IV}]$ had dimensions 0.15 × 0.25 × 0.20 mm. Cell parameters were obtained from 25 reflections with 2θ angles in the range $18.86° < 2\theta < 25.30°$ for $[Et_4N][\mathbf{I}]$, $18.64° < 2\theta < 28.76°$ for $[Et_4N][\mathbf{II}]$, $13.16° < 2\theta < 19.28°$ for $[Et_4N]_2[\mathbf{III}]$, and $22.36° < 2\theta < 29.10°$ for $[Et_4N][\mathbf{IV}]$. A total of 2768 reflections with $I > 2.0\sigma(I)$ for $[Et_4N][\mathbf{I}]$ (1633 reflections with $I > 2.5\sigma(I)$ for $[Et_4N][\mathbf{II}]$, 1680 reflections with $I > 2.0\sigma(I)$ for $[Et_4N]_2[\mathbf{III}]$, and 2687 reflections with $I > 2.5\sigma(I)$ for $[Et_4N][\mathbf{IV}]$) were used in the refinement. The structures were solved by the heavy-atom method and refined by least-squares cycles. All heavy atoms were refined with anisotropic temperature factors. The positions of hydrogen atoms were found from Fourier difference maps. None were refined in the least-squares cycle. Full-matrix least-squares refinement led to convergence with $R = 2.6\%$ and $R_w = 2.5\%$ for $[Et_4N][\mathbf{I}]$, $R = 4.0\%$ and $R_w = 3.4\%$ for $[Et_4N][\mathbf{II}]$, $R = 5.4\%$ and $R_w = 4.9\%$ for $[Et_4N]_2[\mathbf{III}]$, and $R = 4.7\%$ and $R_w = 4.1\%$ for $[Et_4N][\mathbf{IV}]$.

The selected distances and angles of $[Et_4N][\mathbf{I}]$, $[Et_4N][\mathbf{II}]$, $[Et_4N]_2[\mathbf{III}]$, and $[Et_4N][\mathbf{IV}]$ are given in Tables 2−5, respectively. Additional crystallographic data are available as Supporting Information.

Table 4. Selected Bond Distances (Å) and Bond Angles (deg) for $[Et_4N]_2[SFe_2Ru_3(CO)_{14}]$ ($[Et_4N]_2[III]$)[a]

(A) Distances			
Ru(1)−Ru(2)	2.831(3)	Ru(1)−RF	2.766(3)
Ru(1)−FR	2.753(4)	Ru(1)−S	2.447(7)
Ru(2)−RF	2.855(3)	Ru(2)−FR	2.766(4)
Ru(2)−Fe	2.741(4)	RF−Fe	2.698(5)
RF−S	2.396(7)	FR−Fe	2.681(5)
FR−S	2.336(7)	Fe−S	2.238(8)
(B) Angles			
Ru(2)−Ru(1)−RF	61.32(8)	Ru(2)−Ru(1)−FR	59.35(9)
Ru(2)−Ru(1)−S	79.3(2)	RF−Ru(1)−FR	89.5(1)
RF−Ru(1)−S	54.3(2)	FR−Ru(1)−S	53.0(2)
Ru(2)−FR−Fe	60.4(1)	Ru(2)−FR−S	82.6(2)
Fe−FR−S	52.4(2)	Ru(1)−FR−Ru(2)	61.73(9)
Ru(1)−FR−Fe	89.4(1)	Ru(1)−FR−S	56.8(2)
Ru(2)−Fe−RF	63.3(1)	Ru(2)−Fe−FR	61.3(1)
Ru(2)−Fe−S	84.9(2)	RF−Fe−FR	92.5(1)
RF−Fe−S	57.2(2)	FR−Fe−S	55.8(2)
Ru(1)−Ru(2)−RF	58.22(8)	Ru(1)−Ru(2)−FR	58.92(9)
Ru(1)−Ru(2)−Fe	86.6(1)	RF−Ru(2)−FR	87.4(1)
RF−Ru(2)−Fe	57.6(1)	FR−Ru(2)−Fe	58.3(1)
Ru(1)−RF−Ru(2)	60.47(8)	Ru(1)−RF−Fe	88.7(1)
Ru(1)−RF−S	56.1(2)	Ru(2)−RF−Fe	59.1(1)
Ru(2)−RF−S	79.6(2)	Fe−RF−S	51.7(2)
Ru(1)−S−RF	69.6(2)	Ru(1)−S−FR	70.2(2)
Ru(1)−S−Fe	109.2(3)	RF−S−FR	110.3(3)
RF−S−Fe	71.1(2)	FR−S−Fe	71.7(2)

[a] RF = 0.7 Ru + 0.3 Fe and FR = 0.7 Fe + 0.3 Ru.

Table 5. Selected Bond Distances (Å) and Bond Angles (deg) for $[Et_4N][MeSFe_2Ru_3(CO)_{14}]$ ($[Et_4N][IV]$)[a]

(A) Distances			
Ru(1)−Ru(2)	2.874(2)	Ru(1)−RF	2.783(3)
Ru(1)−FR	2.779(3)	Ru(1)−S	2.388(5)
Ru(2)−RF	2.835(2)	Ru(2)−FR	2.768(3)
Ru(2)−Fe	2.751(2)	RF−Fe	2.864(3)
RF−S	2.365(5)	FR−Fe	2.804(3)
FR−S	2.222(6)	Fe−S	2.246(5)
(B) Angles			
Ru(2)−Ru(1)−RF	60.13(5)	Ru(2)−Ru(1)−FR	58.61(7)
Ru(2)−Ru(1)−S	72.9(1)	RF−Ru(1)−FR	90.34(8)
RF−Ru(1)−S	53.8(1)	FR−Ru(1)−S	50.3(1)
Ru(1)−S−RF	71.7(1)	Ru(1)−S−FR	74.1(2)
Ru(1)−S−Fe	119.1(2)	RF−S−FR	118.6(2)
RF−S−Fe	76.8(2)	FR−S−Fe	77.7(2)
Ru(1)−Ru(2)−RF	58.34(6)	Ru(1)−Ru(2)−FR	58.98(7)
Ru(1)−Ru(2)−Fe	90.50(7)	RF−Ru(2)−FR	89.48(7)
RF−Ru(2)−Fe	61.66(6)	FR−Ru(2)−Fe	61.06(7)
Ru(1)−RF−Ru(2)	61.52(6)	Ru(1)−RF−Fe	90.07(8)
Ru(1)−RF−S	54.5(1)	Ru(2)−RF−Fe	57.72(6)
Ru(2)−RF−S	74.0(1)	Fe−RF−S	49.8(1)
Ru(1)−FR−Ru(2)	62.41(6)	Ru(1)−FR−Fe	91.40(9)
Ru(1)−FR−S	55.7(1)	Ru(2)−FR−Fe	59.17(6)
Ru(2)−FR−S	77.4(1)	Fe−FR−S	51.5(1)
Ru(2)−Fe−RF	60.62(6)	Ru(2)−Fe−FR	59.77(7)
Ru(2)−Fe−S	77.4(1)	RF−Fe−FR	88.20(9)
RF−Fe−FR	88.20(9)	RF−Fe−S	53.5(1)

[a] RF = 0.7 Ru + 0.3 Fe and FR = 0.7 Fe + 0.3 Ru.

Results and Discussion

Synthesis and Reactivity of $[SFe_3(CO)_9]^{2-}$. The tetrahedral cluster anion $[SFe_3(CO)_9]^{2-}$ is known and is isostructural with its analogs $[EFe_3(CO)_9]^{2-}$ (E = O, Se, Te).[3c,6,12,13] Several synthetic routes have been

---

(8) North, A. C. T.; Philips, D. C.; Mathews, F. S. *Acta Crystallogr.* **1968**, *A24*, 351.

(9) Gabe, E. J.; Lepage, Y.; Charland, J. P.; Lee, F. L.; White, P. S. *J. Appl. Crystallogr.* **1989**, *22*, 384.

(10) *International Tables for X-ray Crystallography*; Kynoch Press: Birmingham, England, 1974; Vol. IV.

(11) Ceriotti, A.; Resconi, L.; Demartin, F.; Longoni, G.; Manassero, M.; Sansoni, M. *J. Organomet. Chem.* **1983**, *249*, C35.

(12) Bachman, R. E.; Whitmire, K. H. *Inorg. Chem.* **1994**, *33*, 2527.

(13) (a) Voss, E. J.; Stern, C. L.; Shriver, D. F. *Inorg. Chem.* **1994**, *33*, 1087. (b) Schauer, C. K.; Harris, S.; Sabat, M.; Voss, E. J.; Shriver, D. F. *Inorg. Chem.* **1995**, *34*, 5017.

Scheme 1

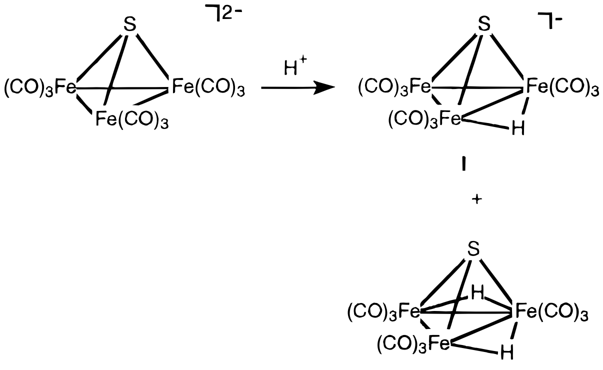

Scheme 2

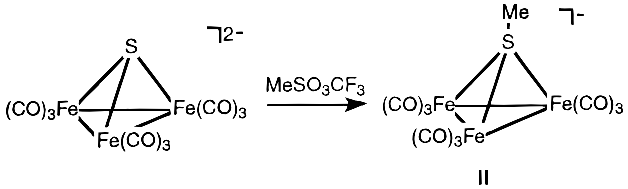

reported; however, these preparations either result in complex mixtures of products or need special reaction conditions.[5] We develop a facile synthesis of $[SFe_3(CO)_9]^{2-}$ by the treatment of Na_2SO_3 with $Fe(CO)_5$/KOH in refluxing methanol solution. The yield is moderate but requires milder conditions. If the reaction was not conducted in basic solution, the monohydrido cluster $[SFe_3(\mu\text{-}H)(CO)_9]^-$ (**I**) would be produced along with the major product $[SFe_3(CO)_9]^{2-}$.

As expected, the acidification of $[SFe_3(CO)_9]^{2-}$ forms the monohydrido cluster $[SFe_3(\mu\text{-}H)(CO)_9]^-$ (**I**) and the dihydrido cluster $SFe_3(\mu\text{-}H)_2(CO)_9$. $SFe_3(\mu\text{-}H)_2(CO)_9$ has been reported to be generated from acidification of the reaction mixture of Na_2S and $Fe(CO)_5$/KOH in MeOH/H_2O solutions, and hydrogen abstraction of $SFe_3(\mu\text{-}H)_2(CO)_9$ leads to the formation of cluster **I**[5a] (Scheme 1). Our method provides a more convenient route to prepare cluster **I**. X-ray analysis of **I** showed that the hydrogen atom bridges one Fe−Fe bond due to the longer bond length, and the ^1H NMR spectrum gives the hydride resonance at −22.93 ppm, to further confirm the presence of the hydrogen atom.[5a] This result is parallel to those found for the acidification of the analogous clusters $[EFe_3(CO)_9]^{2-}$ (E = Se, Te).[6] It is possible that the metal-bridging hydride could be the thermodynamic product resulting from the protonation at the apical sulfur followed by hydride migration. However, the low solubility of these salts prevents a low-temperature NMR study which could probably resolve this question.

To test the basicity of the sulfur atom, we treated $[SFe_3(CO)_9]^{2-}$ with $MeSO_3CF_3$, and the sulfur-methylated product $[MeSFe_3(CO)_9]^-$ (**II**) was obtained (Scheme 2). The ^1H NMR of $[Et_4N]$[**II**] shows the resonance at 2.73 ppm corresponding to the absorption of the methyl group, and the ^{13}C NMR spectrum shows a single CO peak at 218.5 ppm at room temperature. It has been known that the oxygen atom of $[OFe_3(CO)_9]^{2-}$ shows affinity toward both H^+ and Me^+.[11] Our results indicate that the sulfur atom of $[SFe_3(CO)_9]^{2-}$ does show affinity toward Me^+ but not for H^+, probably due to the weaker S−H bond versus O−H bond. It has been shown by Shriver's research group that $[SFe_3(CO)_9]^{2-}$ can react with $[Mn(CO)_3(MeCN)_3]^+$ or $[Re(CO)_5]^+$ to form the μ_4-sulfido clusters $[Fe_3(CO)_9(\mu_4\text{-}S)M(CO)_5]^-$ (M = Mn, Re).[13] $[SFe_3(CO)_9]^{2-}$ was also reported to react with alkyl halides, followed by acidification, to form the complexes $HFe_3(CO)_9(SR)$.[14] In this study, $[SFe_3(CO)_9]^{2-}$ shows a similar affinity toward the Lewis acid Me^+ to form the sulfur-methylated cluster **II**.

Scheme 3

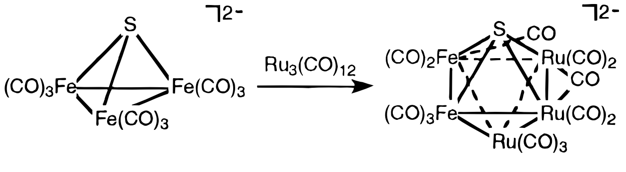

Since the protonation occurred at the Fe-Fe bonds of $[SFe_3(CO)_9]^{2-}$, we wondered whether methylenation gave similar results. To answer this, we treated $[SFe_3(CO)_9]^{2-}$ with the electrophile CH_2I_2. However, this reaction gave the monohydrido cluster **I** instead of the methylenation product. This result is in contrast with the outcomes of the analogous reactions of $[EFe_3(CO)_9]^{2-}$ (E = Se, Te) with the electrophile CH_2I_2.[3g,15] In the Se case, the planar cluster $Se_2Fe_2(CO)_6(CH_2)_2$ was obtained, in which two methylene groups bridge two Se−Fe bonds, whereas in the Te case a similar reaction yielded the butterfly cluster $Fe_2(CO)_6(\mu\text{-}TeCH_2Te)$. We believe this difference may be due to the differing affinities of the clusters $[EFe_3(CO)_9]^{2-}$ toward CH_2I_2.

When the tetrahedral cluster $[SFe_3(CO)_9]^{2-}$ was treated with $Ru_3(CO)_{12}$ in refluxing acetone solution, the octahedral cluster $[SFe_2Ru_3(CO)_{14}]^{2-}$ (**III**) was obtained (Scheme 3). The IR spectrum of $[Et_4N]_2$[**III**] showed terminal carbonyl absorptions in the range 2029−1917 cm^{-1} and a weak peak at 1763 cm^{-1} characteristic of the doubly bridging carbonyl groups. The ESI mass spectrum gives the negative ion peak at *m*/2*e* 420 with an isotope distribution consistent with the formula of **III**. The ^{13}C NMR spectrum shows only a single CO peak at 209.9 ppm, which indicates that the CO groups are undergoing complete site exchange between the metal atoms at ambient temperatures in solution.

The formation of **III** could be regarded as resulting from the $Fe(CO)_3$ vertex loss followed by the combination of the resultant species "SFe_2" with the incoming fragment $Ru_3(CO)_{10}(Me_2CO)_2$. Apparently, the destruction of $[SFe_3(CO)_9]^{2-}$ occurs to accommodate the large metal fragment. This result is similar to those found in the analogous reactions of $[EFe_3(CO)_9]^{2-}$ (E = Se, Te) with $Ru_3(CO)_{12}$.[3g,15] With this study, the class of octahedral clusters with the formula $[(\mu_4\text{-}E)Fe_2Ru_3(CO)_{14}]^{2-}$ (E = O, S, Se, Te) is complete.[3g,15,16] The study indicates that the presence of the differing chalcogen atoms has no significant influence on the formation of the octahedral clusters $[(\mu_4\text{-}E)Fe_2Ru_3(CO)_{14}]^{2-}$.

Since **III** displays an octahedral core with a μ_4-S atom and two bridging CO groups, we wondered whether the μ_4-S atom or the μ-CO group can be alkylated by $MeSO_3CF_3$. The basicity of μ_2- and μ_3-carbonyl oxygen atoms

---

(14) Takács, J.; Markó, L. *Transition Met. Chem.* **1985**, *10*, 21.
(15) Shieh, M.; Cherng, J.-J. Unpublished results.
(16) Schauer, C. K.; Shriver, D. F. *Angew. Chem., Int. Ed. Engl.* **1987**, *26*, 255.

Scheme 4

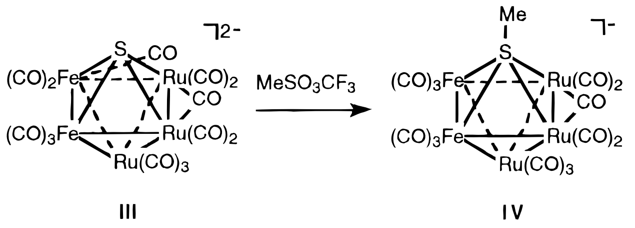

has been well-established,[17] and the μ_4-S bonding mode has also been exploited widely.[4b,18] However, the capability of the μ_4-S atom to serve as a Lewis donor has rarely been seen. The reported examples include $Os_5(CO)_{15}(\mu_5\text{-}S)[W(CO)_4(PPh_3)]$, $Ru_4(CO)_7(PMe_2Ph)_2(\mu\text{-}CO)_2(\mu_4\text{-}S)(\mu_5\text{-}S)\{W(CO)_4PMe_2Ph\}$, and $Ru_4(CO)_{10}\{C(Ph)NMe_2\}(\mu_4\text{-}S)(\mu_5\text{-}S)W(CO)_5$.[19-21] To test the basic site of **III**, we treated $[Et_4N]_2$[**III**] with the methylation agent $MeSO_3CF_3$. Interestingly, the sulfur-methylated product $[Et_4N][MeSFe_2Ru_3(CO)_{14}]$ ($[Et_4N]$[**IV**]) was obtained (Scheme 4).

The CO absorption pattern of **IV** is similar to that for cluster **III**, but it is shifted about 30 cm^{-1} to higher frequencies. X-ray analysis confirms that **IV** retains the octahedral core geometry with the sulfur atom externally bonded to a methyl group. The ESI mass spectrum gives the negative ion peak at m/e 856 with the isotope distribution consistent with three Ru atoms. The ^1H NMR spectrum of the methyl group appears at 2.36 ppm, which is similar to that found for cluster **II**. A single CO peak at 205.2 ppm was observed in the ^{13}C NMR spectrum of **IV**, which indicates that the CO groups are undergoing complete site exchange between the metal atoms at ambient temperatures in solution. Cluster **IV** represents an example of a μ_4-S atom acting as a Lewis donor. In comparison to the methylation of $[SFe_3(CO)_9]^{2-}$, once again, the sulfur atoms of these clusters show affinity toward the Lewis acid Me^+ due to their pronounced basicity.

The reactions of $[SFe_3(CO)_9]^{2-}$ with electrophiles are summarized in Scheme 5.

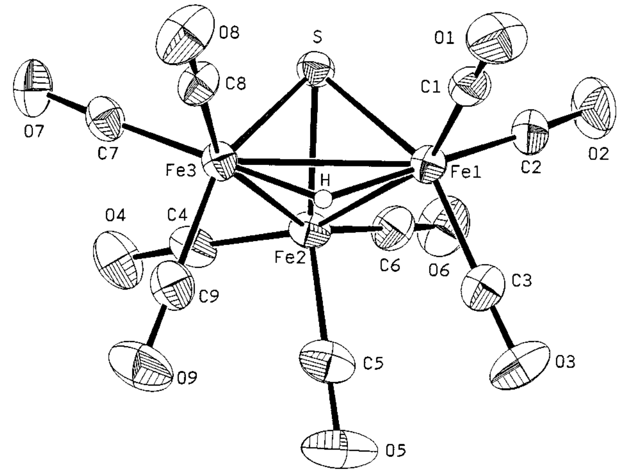

Figure 1. ORTEP diagram of $[SFe_3(\mu\text{-}H)(CO)_9]^-$ (**I**). Thermal ellipsoids are drawn at the 30% probability level.

Scheme 5

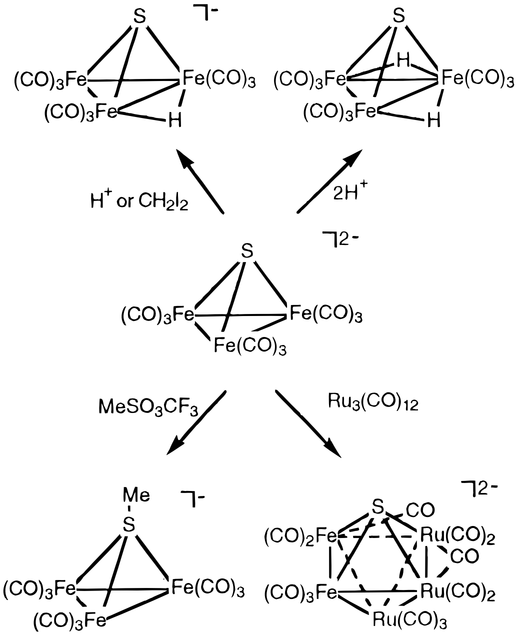

Crystal Structures of $[Et_4N]$[I], $[Et_4N]$[II], $[Et_4N]_2$[III], and $[Et_4N]$[IV]. The core of **I** displays a tetrahedral geometry with one μ_3-S atom and one Fe—Fe bond bridging by a hydrogen atom. The ORTEP diagram was shown in Figure 1. The S—Fe distances average 2.196 Å with very little variation (2.191(1) Å—2.203(1) Å), which are close to those in the clusters $S_2Fe_2(CO)_6$ (aveerage 2.228 Å)[22] and $SFe_3(CO)_9\{Au_2(PPh_3)_2\}$ (average 2.203 Å).[5c] In contrast, the Fe—Fe distances (2.5730(9), 2.668(1), and 2.580(1) Å) show a larger variation. The longest Fe—Fe bond is bridged by a hydride atom, where Fe—H distances of 1.63(3) and 1.52(3) Å are found. The lengthening of the Fe—Fe bond is due to the bridging ligand, which is also seen in the related cluster $SFe_3(CO)_9\{Au_2(PPh_3)_2\}$.[5c]

The metal core of **II** is similar to that of cluster **I**. As shown in Figure 2, cluster **II** contains a mirror plane going through S, Fe(2), and the center of the Fe(1)—Fe(1a) bond. Cluster **II** is structurally analogous to $[t\text{-}BuSFe_3(CO)_9]^-$.[23] In **II**, the S—Fe distances average 2.126 Å, close to those for $[t\text{-}BuSFe_3(CO)_9]^-$ (2.120 Å) and $[Fe_3(CO)_9(SO)]^{2-}$ (2.132 Å).[24] The Fe—Fe distances are similar and average 2.637 Å, which is similar to 2.644 Å in $[t\text{-}BuSFe_3(CO)_9]^-$ but a bit longer than those found in other S—Fe clusters such as $S_2Fe_2(CO)_6$ (2.552(2) Å),[22] $(SEt)_2Fe_2(CO)_6$ (2.54(1) Å),[25] and $\{Fe_2(CO)_6(\mu\text{-}SMe)\}_2S$ (2.540(6) Å).[26] The S—C length of 1.836(7) Å is normal.

---

(17) Horwitz, C. P.; Shriver, D. F. *Adv. Organomet. Chem.* **1984**, *23*, 219.

(18) (a) Whitmire, K. H. *J. Coord. Chem.* **1988**, *17*, 95. (b) Adams, R. D.; Babin, J. E.; Tasi, M. *Inorg. Chem.* **1987**, *26*, 2807. (c) Adams, R. D.; Babin, J. E.; Tsai, M. *Inorg. Chem.* **1986**, *25*, 4460. (d) Adams, R. D.; Babin, J. E.; Tsai, M. *Inorg. Chem.* **1986**, *25*, 4514.

(19) Adams, R. D.; Babin, J. E.; Natarajan, K. *J. Am. Chem. Soc.* **1986**, *108*, 3518.

(20) Adams, R. D.; Babin, J. E.; Wang, J.-G. *Polyhedron* **1989**, *8*, 2351.

(21) Adams, R. D.; Babin, J. E.; Natarajan, K.; Tsai, M.; Wang, J. G. *Inorg. Chem.* **1987**, *26*, 3708.

(22) Wei, C. H.; Dahl, L. F. *Inorg. Chem.* **1965**, *4*, 1.

(23) (a) Winter, A.; Zsolnai, L.; Huttner, G. *Chem. Ber.* **1982**, *115*, 1286. (b) Winter, A.; Zsolnai, L.; Huttner, G. *J. Organomet. Chem.* **1983**, 409.

(24) Karet, G. B.; Stern, C. L.; Norton, D. M.; Shriver, D. F. *J. Am. Chem. Soc.* **1993**, *115*, 9979.

(25) Dahl, L. F.; Wei, C. H. *Inorg. Chem.* **1963**, *2*, 328.

(26) Coleman, J. M.; Wojcicki, A.; Pollick, P. J.; Dahl, L. F. *Inorg. Chem.* **1967**, *6*, 1236.

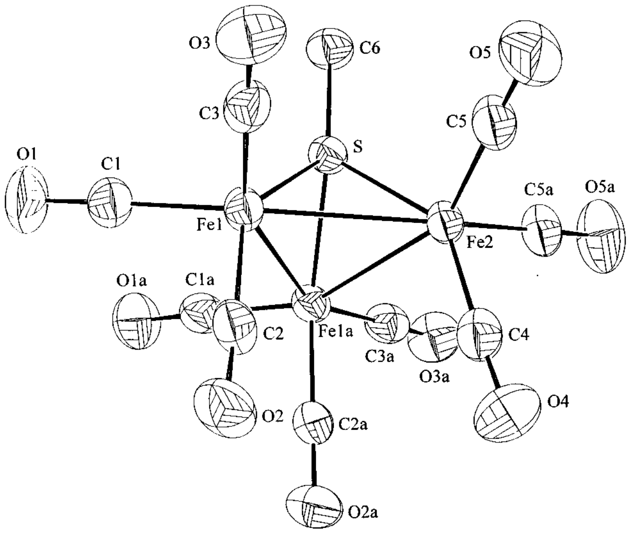

Figure 2. ORTEP diagram of $[MeSFe_3(CO)_9]^-$ (**II**). Thermal ellipsoids are drawn at the 30% probability level.

Clusters **I** and **II** are structurally similar to the previously characterized cluster $[SFe_3(CO)_9]^{2-}$.[27] Other related (μ_3-S)M_3 clusters are also found for $SFeCo_2(CO)_9$,[5c] $SFe_2Co(CO)_8(NO)$,[5c] and $FeCo_2(CO)_9\{\mu_3\text{-}SCr(CO)_5\}$.[28] It is found that the average S−Fe distance of cluster **I** (2.196 Å) is very close to that of $[SFe_3(CO)_9]^{2-}$ (2.190 Å) but longer than that of **II** (2.126 Å). However, the average Fe−Fe distances of **I** and **II** (2.607, 2.637 Å) are significantly larger than that found for $[SFe_3(CO)_9]^{2-}$ (2.584 Å), indicative of the dispersion of electron density to the incoming species H^+ and Me^+.

Cluster **III** displays an octahedral metal core with a μ_4-S atom and two carbonyl groups bridging one Ru−Ru and one Ru−Fe bond (Figure 3). The sulfur atom acts as a four-electron donor to the Fe_2Ru_3 metal core, which obeys Wade's rule for a six-vertex *closo* cluster possessing seven skeletal bonding pairs. Cluster **III** is structurally similar to its analogs $[EFe_2Ru_3(CO)_{14}]^{2-}$ (E = O, Se).[3g,16] X-ray analysis shows that it is not possible to distinguish the positions of one Ru and one Fe atom. However, the formulation of **III** was substantiated by elemental analyses and negative ion mass spectroscopy. The core geometry of **IV** is similar to that of **III**, except that the sulfur atom is methylated in cluster **IV** (Figure 4). The interesting difference is that cluster **IV** has only one μ_2-carbonyl bridging one Ru−Ru bond whereas **III** possesses two μ_2-carbonyls bridging one Ru−Fe and one Ru−Ru bonds. The absence of one bridging carbonyl in **IV** could be attributed to the neutralization of the negative charge from 2− to 1− by the methyl group.

For comparison, the S-Fe distance of 2.238(8) Å in cluster **III** is similar to 2.246(5) Å in cluster **IV** and larger than those found in tetrahedral clusters **I**, **II**, and $[SFe_3(CO)_9]^{2-}$. The S−Ru(1) length of 2.447(7) Å in **III** and that of 2.388(5) Å in **IV** are within the ranges of the reported S−Ru distances in related clusters such as $(\mu_4\text{-}S)_2(\eta\text{-tol})Ru_8(CO)_{17}$,[18c] $(\mu_4\text{-}S)_2Ru_4(CO)_9(PMe_2Ph)_2$,[18d] $Ru_6(CO)_{17}(\mu_4\text{-}S)_2$, and $Ru_5(CO)_{14}(\mu_4\text{-}S)_2$.[18b] The unbridged Ru(1)−Ru(2) distances in **III** and **IV** (2.831(3) and 2.874(2) Å) are close to those in $Ru_3(CO)_{12}$ (2.852−2.859 Å).[29]

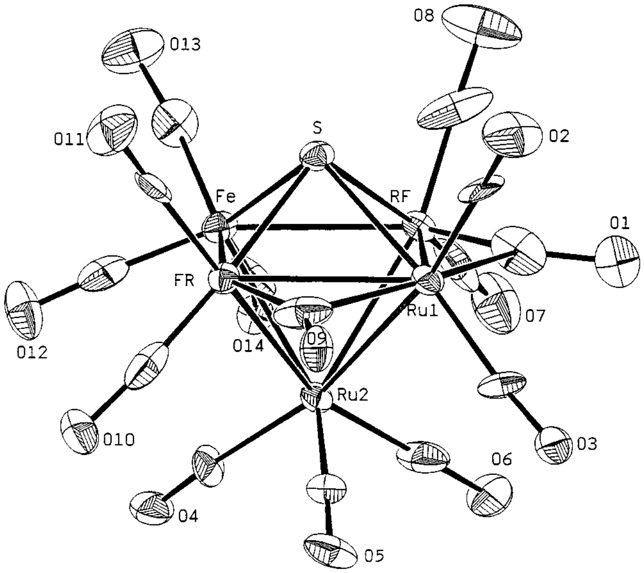

Figure 3. ORTEP diagram of $[SFe_2Ru_3(CO)_{14}]^{2-}$ (**III**) (where RF = 0.7 Ru + 0.3 Fe and FR = 0.7 Fe + 0.3 Ru). The labels for the carbon atoms are omitted for clarity. Thermal ellipsoids are drawn at the 30% probability level.

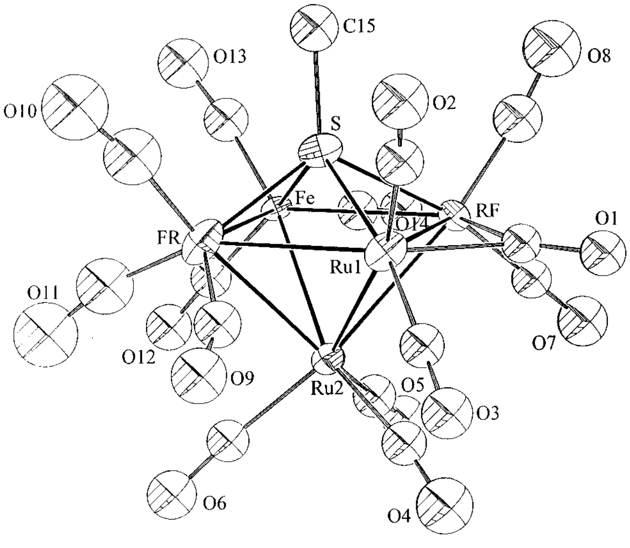

Figure 4. ORTEP diagram of $[MeSFe_2Ru_3(CO)_{14}]^-$ (**IV**) (where RF = 0.7 Ru + 0.3 Fe and FR = 0.7 Fe + 0.3 Ru). The labels for the carbon atoms of the carbonyls are omitted for clarity. Thermal ellipsoids are drawn at the 30% probability level.

Conclusion

We have developed a convenient route to the tetrahedral cluster $[(\mu_3\text{-}S)Fe_3(CO)_9]^{2-}$, which shows affinity toward the electrophiles H^+, Me^+, and $Ru_3(CO)_{10}(Me_2CO)_2$. It has been demonstrated that the basic sites of this cluster are located either between Fe−Fe bonds or at the sulfur atom, depending on the different electrophiles H^+ and Me^+. In the case of the reaction of $[(\mu_3\text{-}S)Fe_3(CO)_9]^{2-}$ with $Ru_3(CO)_{12}$, the whole cluster should

---

[27] (a) Fischer, K.; Deck, W.; Schwarz, M.; Vahrenkamp, H. *Chem. Ber.* **1985**, *118*, 4946. (b) Al-Ani, F. T.; Hughes, D. L.; Pickett, C. J. *J. Organomet. Chem.* **1986**, *307*, C31.

[28] Richter, F.; Vahrenkamp, H. *Angew. Chem., Int. Ed. Engl.* **1978**, *17*, 444.

[29] Churchill, M. R.; Hollander, F. J.; Hutchinson, J. P. *Inorg. Chem.* **1977**, *16*, 2655.

be taken into consideration. The μ_4-S atom in the resultant octahedral cluster $[(\mu_4\text{-S})Fe_2Ru_3(CO)_{14}]^{2-}$ shows pronounced basicity toward the Lewis acid Me^+.

Acknowledgment. We thank the National Science Council of the Republic of China for financial support (Grant No. NSC 85-2113-M-003-003).

Supporting Information Available: Complete listings of crystallographic data, atomic positional parameters, bond distances and angles, and anisotropic thermal parameters for the complexes $[Et_4N]$[**I**], $[Et_4N]$[**II**], $[Et_4N]_2$[**III**], and $[Et_4N]$[**IV**] (22 pages). Ordering information is given on any current masthead page.

OM970710M